

Estimating Retrosensor Position from Range Data

A. W. Merz*

Lockheed Missiles & Space Company,
Palo Alto, California 94304

Introduction

A RETROREFLECTOR returns a signal that depends on its distance from a laser beam passing nearby. It acts as a passive mirror, returning a signal to a sensor mounted near the source of the beam, at a considerable range. The retroreflector is located in the x, y plane, as shown in Fig. 1. This plane is normal to the marker beam nominal direction, and the beam describes a circle in this plane at a constant rate. The retroreflector is assumed to be at rest during the time required for many cycles of data, and so no dynamic equations or transition matrix are needed for the retro. The two coordinates of the retro are to be estimated. This is done using signal strength or brightness data, which vary with the range of the reflector from the beam. The time variation of this signal strength yields estimates and covariances of the retroreflector coordinates.

Analysis

This signal strength S is supposed to be a normally distributed function of the distance d between marker beam and retroreflector, as shown in Fig. 1. This distance varies with time as the marker beam follows its known circular path about the origin. The signal strength would be constant only if d were constant, i.e., if the reflector were located at the origin. In the general case, the signal strength is,

$$S(d) = S_0 \exp[-0.5(d/\sigma)^2] \quad (1)$$

where σ is the known standard deviation of the beam. The peak probability density of the beam is

$$S_0 = 1/(2\pi\sigma^2) \quad (2)$$

Other known parameters in Fig. 1 are the sensor distance r_0 and the angle A . The data are expressed as

$$\text{data} = S(r, \theta, A) + \text{noise} \quad (3)$$

where the constant coordinates r, θ are to be estimated from a sequence of angles A and the corresponding signals $S(d)$. The covariance of the noise is R .

The range is implied by Eq. (1) in terms of the signal strength, i.e., this equation is inverted to give

$$d^2 = 2\sigma^2 \log(S_0/S) \quad (4)$$

and the law of cosines is used with the triangle in Fig. (1) to yield

$$d^2 = r_0^2 + r^2 - 2rr_0 \cos(A - \theta) \quad (5)$$

Combining these two equations and adding noise, the data are the following function of the signal strength $S(n)$ and the coordinates:

$$z(n) = 2\sigma^2 \log[S_0/S(n)] - r_0^2 + \text{noise} \quad (6)$$

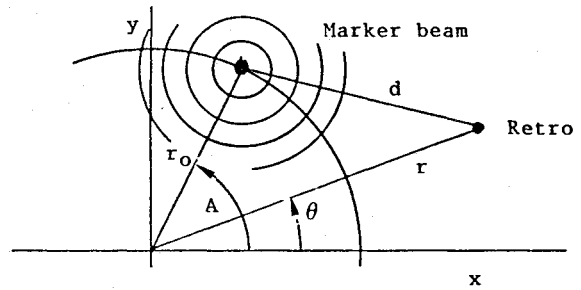


Fig. 1 Marker beam and retrotarget.

$$= r^2 - 2r_0r \cos[A(n) - \theta] + \text{noise} \quad (7)$$

The signal strength and various constants permit computation of the data from Eq. (6), which is the function in Eq. (7) of the coordinates being estimated. The argument $A(n)$ is assumed known, and the noise is assumed of zero-mean and known covariance. The assumption that noise in the signal strength $S(n)$ can be expressed additively as in Eq. (6) may be a poor assumption for small signal-to-noise ratios.

A Kalman filter formulation leads to both estimate and covariance. Linearization gives the error between the actual and the predicted data,

$$dz = z - \hat{z} \approx \left(\frac{dz}{dx} \right) dx + \text{noise} = H dx + \text{noise} \quad (8)$$

where \hat{z} is the estimated value of the data, and the state increment is

$$dx = (dr, d\theta)' \quad (9)$$

The H matrix of Eq. (8) is found to be

$$H(n) = 2\{r - r_0 \cos[A(n) - \theta], -r_0r \sin[A(n) - \theta]\} \quad (10)$$

The updated estimate of the state vector is then,

$$\hat{x}(n) = \hat{x}(n-1) + K(n) dz \quad (11)$$

The difference between the actual noisy data and the predicted data is

$$dz = z(n) - \hat{z}^2 - 2r_0\hat{r}(n) \cos[A(n) - \hat{\theta}(n)]$$

where the estimation gain matrix minimizes the trace of the covariance,

$$V(n) = E\{[x(n) - \hat{x}(n)][x(n) - \hat{x}(n)]'\}$$

The optimal gain vector depends on both the state covariance V and the data covariance R :

$$K(n) = V(n)H'(n)/[H(n)V(n)H'(n) + R] \quad (12)$$

This gain provides the maximum reduction in the trace of the covariance at the time of the data update. The subsequent covariance of the state is

$$V(n+1) = [I - K(n)H(n)]V(n) \quad (13)$$

The data matrix H in Eq. (10) uses the latest estimates for (r, θ) . This estimate of the H matrix is then used in Eq. (12), and the gain is used to update both the estimate and the covariance in Eqs. (11) and (13).

Numerical Example

An example shows typical time variations of the estimates of the retroposition. The data occur at the rate of 5 per marker

Received April 17, 1990; revision received July 13, 1990; accepted for publication July 18, 1990. Copyright © 1990 by the American Institute of Aeronautics and Astronautics, Inc. All rights reserved.

*Staff Scientist, Advanced Systems Studies, Dept. 9220, Bldg. 254E, 3251 Hanover St. Associate Fellow AIAA.

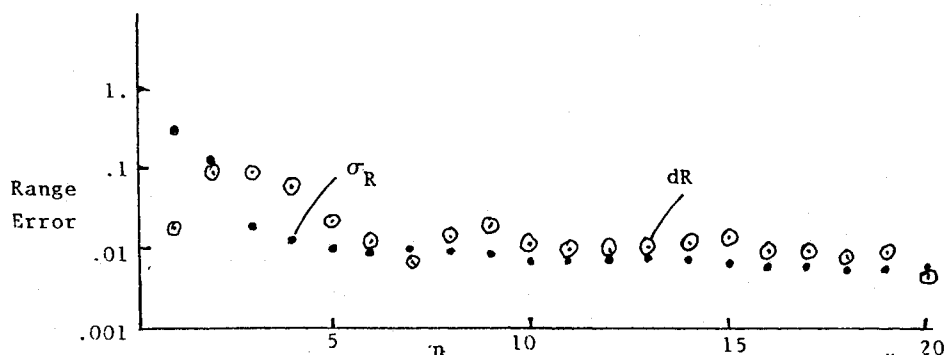


Fig. 2 Range estimation error and standard deviation.

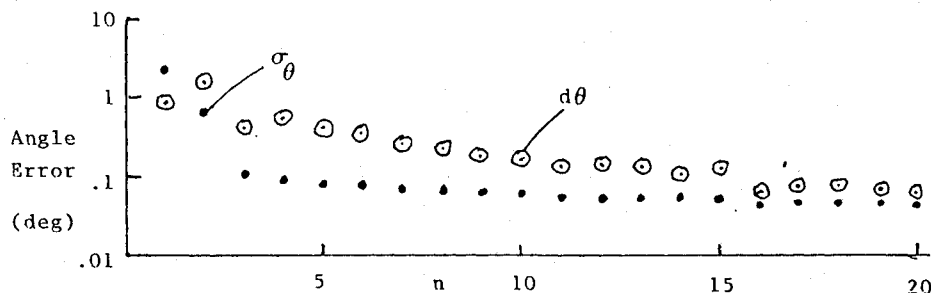


Fig. 3 Azimuth estimation error and standard deviation.

beam cycle, therefore A varies by 72 deg between data. The initial estimates $(\hat{r}, \hat{\theta})$ converge toward the actual values. The noise in the data is simulated as having a constant covariance, which may not be the case. If a dependence of noise on range can be estimated or conjectured, the effects of such noise on the estimate can be forecast.

Figures 2 and 3 show the time variations of errors in the estimates of range and azimuth angle, with their rms errors (1σ). Despite large nonlinearities and an indifferent initial estimate, the convergence is rapid and the errors ($d\hat{r}, d\hat{\theta}$) are consistent with the estimated standard deviations. In an actual application, of course, the errors are not known and the standard deviations are found, as in this example.

Conclusions

Filter techniques have been applied to an estimation problem for a nonlinear, time-varying parameter system. The process yields estimates and rms errors that are consistent and well-behaved functions of the noisy data. The data in the example have been chosen to highlight the filter characteristics and do not apply to any current physical system.

Dominance of Stiffening Effects for Rotating Flexible Beams

C. Smith* and H. Baruh†

Rutgers University, Piscataway, New Jersey 08855

Introduction

SEVERAL proposed approaches to the derivation of the equations of motion for rotating flexible beams are essentially similar in the linear terms of the generalized coordinates

Received Feb. 27, 1990; revision received July 16, 1990; accepted for publication July 17, 1990. Copyright © 1990 by the American Institute of Aeronautics and Astronautics, Inc. All rights reserved.

*Graduate Student, Department of Mechanical and Aerospace Engineering; currently, Aerospace Engineer, Federal Aviation Administration, Pomona, NJ. Member AIAA.

†Associate Professor, Department of Mechanical and Aerospace Engineering, P.O. Box 909. Member AIAA.

associated with the elastic motion. All methods include the two opposing effects often referred to as *geometric stiffening* and *centrifugal softening*.¹ (Since this nomenclature is not accepted universally, we shall refer to these effects as simply stiffening and softening.) The softening effect, being purely the result of kinematics in a rotating frame, is the easiest to identify.

The stiffening effect is somewhat more complicated. Reference 1 shows that the stiffening can be interpreted as being the result of a quasisteady longitudinal strain. Reference 2 shows that the stiffening can be derived from consideration of an effect known as *foreshortening*. Other approaches^{3,4} introduce an angular-velocity dependent component to the potential energy. All of these efforts are motivated by the desire to retain the computational simplicity of the Euler-Bernoulli beam theory. Other authors, including most recently Hanagud and Sarkar,⁵ insist that the centrifugal stiffening effect can (and should) be derived from the nonlinear beam theory.

We show here that, for a class of beams rotating in a plane, the stiffening effect always dominates the softening effect. Although it seems intuitively obvious that a flexible beam rotating in a plane will always stiffen, a proof of this has not yet been presented. It is expected that this proof will also serve as a vehicle for further results.

Proof that Geometrical Stiffening Dominates Centrifugal Softening

The results presented are valid for any boundary conditions. For the case of a free-free beam, the flexible motion is described with respect to a rotating reference frame whose origin coincides with the center of mass of the beam. For the pinned-free and fixed-free cases, the origin of the rotating reference frame coincides with the pinned or fixed end of the beam. In both cases, we assume that there is no external axial force on the beam.

Consider a beam of arbitrary mass and stiffness distributions whose elastic axis and centroidal axis coincide and assume the constraint used to determine the angular velocity ω of the reference frame is not affected by the modal coordinates associated with elastic deformation. Let the total displacement of any point on the beam be $r(x, t) = \hat{r}(t) + xi + u(x, t)j$, and let the angular velocity be $\omega(t) = \omega(t)k$ (Fig. 1), where $\hat{r}(t)$ locates the center of mass for the free-free case. The elastic